Origins of 210 Pb- 226 Ra disequilibria in basalts: New insights from the 1978 Asal Rift eruption

Simon Turner, Mark Reagan, Nathalie Vigier, Bernard Bourdon

Geochemistry Geophysics Geosystems G3

Article
Volume 13, Number 7
6 July 2012
Q07002, doi:10.1029/2012GC004173
ISSN: 1525-2027

Published by AGU and the Geochemical Society

Origins of ^{210}Pb-^{226}Ra disequilibria in basalts: New insights from the 1978 Asal Rift eruption

Simon Turner
Department of Earth and Planetary Sciences, Macquarie University, Sydney, New South Wales 2109, Australia (simon.turner@mq.edu.au)

Mark Reagan
Department of Geoscience, University of Iowa, Iowa City, Iowa 52242, USA

Nathalie Vigier
CRPG-CNRS, Nancy Université, B.P. 20, F-54501 Vandoeuvre lès Nancy CEDEX, France

Bernard Bourdon
Laboratoire de Géologie de Lyon, CNRS, UMR 5276, Ecole Normale Supérieure de Lyon, F-69364 Lyon, France

[1] There has been much debate as to whether ^{210}Pb-^{226}Ra disequilibria in young volcanic rocks result from partial melting, cumulate interaction or magma degassing. Here we present new data from basalts erupted in 1978 from Ardoukoba volcano in the Asal Rift. The $(^{210}Pb/^{226}Ra)_t$ ratios are very low (0.2 to 0.6) and appear to correlate negatively with (^{226}Ra/^{230}Th). Invariant (^{230}Th/^{238}U) and (^{231}Pa/^{235}U) ratios require similar melting rates, porosities, and extents for all parental magmas. Thus, the range in (^{226}Ra/^{230}Th), which is negatively correlated with Th concentration, reflects fractional crystallization over millennia after the magmas were emplaced into the crust. This precludes the ^{210}Pb deficits from resulting from partial melting. Instead, the ^{210}Pb deficits must have formed subsequent to magma differentiation and are interpreted to reflect several decades of magma degassing. Many young basalts erupted in a variety of tectonic settings are similarly depleted in ^{210}Pb with respect to ^{226}Ra, suggesting that they continuously degas over a period of a few to several decades, perhaps reflecting the time required to rise to the surface from deeper reservoirs. In some of these basalts, gas accumulation leads to the shallowest, most evolved, and earliest erupting magmas having the highest (^{210}Pb/^{226}Ra) ratios and sometimes ^{210}Pb excesses.

Components: 5000 words, 2 figures, 1 table.

Keywords: Asal Rift; U-series disequilibria; basalt; degassing; differentiation.

Index Terms: 1009 Geochemistry: Geochemical modeling (3610, 8410); 1036 Geochemistry: Magma chamber processes (3618); 1037 Geochemistry: Magma genesis and partial melting (3619).

Received 28 March 2012; **Revised** 4 June 2012; **Accepted** 6 June 2012; **Published** 6 July 2012.

Turner, S., M. Reagan, N. Vigier, and B. Bourdon (2012), Origins of ^{210}Pb-^{226}Ra disequilibria in basalts: New insights from the 1978 Asal Rift eruption, *Geochem. Geophys. Geosyst.*, *13*, Q07002, doi:10.1029/2012GC004173.

1. Introduction

[2] ^{210}Pb disequilibria (half-life = 22.6 years) is common in lavas <100 years old and there has been much interest the ability of this system to constrain magmatic timescales and processes (see Berlo and Turner, 2010, for a recent review). While the origin of ^{210}Pb excess (with respect to its great grandparent ^{226}Ra) is now widely attributed to accumulation of the intermediate gas ^{222}Rn [e.g., *Condomines et al.*, 2010; *Berlo et al.*, 2006; *Reagan et al.*, 2006], the origin of ^{210}Pb deficits is more controversial. *Gauthier and Condomines* [1999] recognized that ^{210}Pb deficits can be produced by magmatic degassing of ^{222}Rn and presented a model to calculate the timescales involved. This model has subsequently been applied to a number of volcanic eruptions [e.g., *Reagan et al.*, 2005, 2006; *Berlo et al.*, 2006; *Turner et al.*, 2004, 2007].

[3] In contrast, *Rubin et al.* [2005] observed a negative correlation between (^{210}Pb/^{226}Ra) and (^{226}Ra/^{230}Th) among young oceanic basalts from the East Pacific Rise, Juan de Fuca Ridge and Loihi and concluded that this resulted from their genesis by partial melting of the mantle. By implication this would require melt extraction from the mantle and migration to the surface within decades [see also *Sigmarsson*, 1996; *McKenzie*, 2000]. Alternatively, *Van Orman and Saal* [2009] have suggested that ^{210}Pb deficits could result from diffusive processes during interaction between melts and cumulates in crustal magma chambers. Finally, fractional crystallization of phases with a greater affinity for Pb over Ra, such as a sulfide, could also potentially lower (^{210}Pb /^{226}Ra) in basaltic melts.

[4] Clearly, it is necessary to distinguish between the above possibilities before the full implications of ^{210}Pb disequilibria for magmatic timescales and processes can be realized. A useful prerequisite is a suite of basalts erupted in a short period in a well-constrained and simple tectonic environment. Accordingly, we present here ^{210}Pb-^{226}Ra data for basalts from the Asal Rift and show how these provide new insights into the origins of such signals and magmatic plumbing systems.

2. The 1978 Eruption of Ardoukoba, Asal Rift

[5] Over the course of a week in November 1978 a series of basaltic lavas flows erupted from Ardoukoba volcano in the central Asal Rift of the African triple junction in Djibouti. This event afforded a rare opportunity to investigate very short-lived U-series disequilibria in basaltic magmas produced by decompression associated with rifting – somewhat like a subaerial analogue of a nascent mid-ocean ridge. Eruption was accompanied, and followed, by ~2 months of significant seismic activity and normal faulting inferred to be related to magma injection in the form of dykes [*Jacques et al.*, 1996]. Geophysical data suggest the existence of a single, southeast-dipping, magma chamber at ~2–4 km depth beneath the Asal Rift [*Van Ngoc et al.*, 1981]. The lavas were extruded along fissures that migrated from northwest to southeast over the week and the samples reported in Table 1 are ordered in eruption sequence from earliest to latest. All of the samples were collected within days of the eruption and are very fresh, highly vesicular, plagioclase-phyric basalts containing minor olivine and clinopyroxene. *Vigier et al.* [1999] inferred that the lavas had accumulated ~30% plagioclase.

[6] Major and trace element data, along with Sr and U-Th-Pa-Ra isotope data for a suite of samples from the eruption were presented by *Vigier et al.* [1999]. They found that ^{87}Sr/^{86}Sr, (^{230}Th/^{232}Th), (^{230}Th/^{238}U), and (^{231}Pa/^{235}U) ratios are largely invariant (Figures 1a and 1b) but that (^{226}Ra/^{230}Th) ratios ranged from 1.93 to 1.35 (Figure 1c). *Vigier et al.* [1999] used these data to infer minimum differentiation timescales for several related magma batches ranging from 320 to 2570 or 650 to 6730 years, using closed- and open-system fractional crystallization models, respectively. The magma residence times were related to the extent of fractional crystallization as reflected in concentrations of highly incompatible elements (e.g., Th), such that the longest residence times were inferred for the most evolved magmas which were the first erupted, whereas shorter residence times were inferred for the less evolved magmas that erupted last.

3. Analytical Techniques

[7] The materials analyzed here were aliquots of the same whole rock powders used by *Vigier et al.* [1999] to which the reader is referred for additional details and bulk compositional data. Replicate trace element and U-series analyses performed by *Vigier et al.* [1999] demonstrate the homogeneity of the powders, even between different samples from the same flow.

[8] In order to complete the ^{226}Ra data reported by *Vigier et al.* [1999], sample 546 was analyzed for

Table 1. ^{226}Ra and ^{210}Pb Data for 1978 Asal Rift Samples in Order of Eruptive Sequence (Earliest to Latest)[a]

Sample	SiO_2 (wt. %)	^{226}Ra (fg/g)	^{210}Pb (dpm/g)	(^{210}Pb/^{226}Ra)	(^{210}Pb/^{226}Ra)$_t$	Degassing Duration[b] (yr)
544	*48.53*	*166.9 ± 3.0*	0.306 ± 0.018	0.834 ± 0.062	0.56 ± 0.15[c]	19
545	*47.81*	*117.9 ± 2.1*	0.199 ± 0.014	0.768 ± 0.073	0.38 ± 0.16[c]	31
DP13	*47.40*	*100.9 ± 1.8*	0.161 ± 0.012	0.726 ± 0.077	0.27 ± 0.16[c]	43
547	*47.35*	*102.4 ± 1.8*	0.160 ± 0.012	0.711 ± 0.078	0.23 ± 0.16[c]	48
546	*47.47*	98.1 ± 1.8	0.157 ± 0.010	0.728 ± 0.066	0.28 ± 0.14[c]	42

[a]Data in italics are from *Vigier et al.* [1999]. ^{226}Ra measurements followed methodology described in *Vigier et al.* [1999] and *Turner et al.* [2000]. (^{210}Pb) values were based on (^{210}Po) measurements performed in 2010 and 2011 following the methodology described in *Reagan et al.* [2006]. (^{210}Pb/^{226}Ra)$_t$ values were corrected for 32 to 33 years of radioactive equilibration. Errors are 2σ.
[b]Degassing durations calculated following *Gauthier and Condomines* [1999] assuming, F = 1.
[c]Errors propagated for the 32 to 33 year interval between eruption and analysis.

^{226}Ra at Macquarie University following chemical separation and analytical methodologies described in *Turner et al.* [2000], which are essentially the same as those used by *Vigier et al.* [1999]. For the purposes of this paper, the ^{226}Ra concentration errors for all the samples are assumed to be no better than that quoted for the NIST 4969 ^{226}Ra standard (±1.8%) against which the ^{228}Ra spikes were calibrated, even though within run errors were typically ≤0.5% [see also *Vigier et al.*, 1999].

[9] The (^{210}Pb) values are based on (^{210}Po) measurements preformed at the University of Iowa in 2010 and 2011 following the methodology described in *Reagan et al.* [2006]. Errors quoted in Table 1 are 2σ. (^{210}Po) measured for BCR-2 at the same time as the samples was 1.26 ± 0.05 dpm/g. Initial (^{210}Pb/^{226}Ra)$_t$ ratios were corrected for the 32 to 33 year interval between eruption and analysis according to the equation (^{210}Pb/^{226}Ra)$_t$ = 1 + [(^{210}Pb/^{226}Ra) − 1] · $e^{\lambda Pbt}$. The age propagated error on the (^{210}Pb/^{226}Ra)$_t$ ratio was thus expanded to be the error on the calculated (^{210}Pb/^{226}Ra) ratio, calculated as ((^{210}Pb/^{226}Ra) × √((err Ra/Ra$_{meas}$ ^2) + (err Po/Po$_{meas}$ ^2))), multiplied by $e^{\lambda Pbt}$ [see also *Condomines et al.*, 2010].

4. Results

[10] Table 1 presents our new ^{226}Ra (sample 546) and ^{210}Pb data to complement the data set provided by *Vigier et al.* [1999]. Figure 1c shows that the calculated (^{226}Ra/^{230}Th) ratio for sample 546 conforms to the negative correlation between (^{226}Ra/^{230}Th) and Th concentration originally observed by *Vigier et al.* [1999]. The measured ^{210}Pb activities vary from 0.31 to 0.16 dpm/g and the resultant eruption age-corrected (^{210}Pb/^{226}Ra)$_t$ ratios range from 0.56 ± 0.15 to 0.20 ± 0.16. These are lower than observed in most volcanic rocks [*Berlo and Turner*, 2010]. Overall, the (^{210}Pb/^{226}Ra)$_t$ ratios largely overlap within error. However, as shown in Figure 2a, the most probable values correlate negatively with (^{226}Ra/^{230}Th) and overall decrease from earliest to latest erupted lava (see Table 1). SiO_2 contents and the overall extent of fractional crystallization, as indicated by the abundances of incompatible elements like Th (Figures 1c and 2b) and Rb (not plotted), also decreased during the course of the eruption *Vigier et al.* [1999]. In the following discussion, we sequentially examine possible models for the origin of the large ^{210}Pb deficits that are observed in all of the Asal lavas. We then consider the wider implications of the data for current models for the timescales of basaltic processes.

5. Origin Through Partial Melting?

[11] Although the absolute magnitude of the (^{210}Pb/^{226}Ra)$_t$ and (^{226}Ra/^{230}Th) ratios are lower and higher, respectively, than the oceanic basalt data presented by *Rubin et al.* [2005], the relationship between (^{210}Pb/^{226}Ra)$_t$ and (^{226}Ra/^{230}Th) in Figure 2a is the same (excluding 2 samples, the oceanic data have (^{210}Pb/^{226}Ra)$_t$ = 0.86–1.1 and (^{226}Ra/^{230}Th) = 1.9–2.9, respectively). For a typical mantle peridotite assemblage the bulk partition coefficients for all of the elements in the U decay-series are <0.01, and the order of compatibility is Pb > U > Th ≫ Pa > Ra [e.g., *Blundy and Wood*, 2003] and so mantle melting should lead to deficits in ^{210}Pb combined with excesses in ^{226}Ra. Using parameters appropriate to the Asal Rift situation, a simple dynamic melting model [*Williams and Gill*, 1989] can simulate the range in (^{226}Ra/^{230}Th) ratios by varying porosity during melting, although it predicts slightly lower (^{210}Pb/^{226}Ra) ratios than observed (Figure 2a). This difference between measured and observed (^{210}Pb/^{226}Ra)$_t$ ratios could easily be

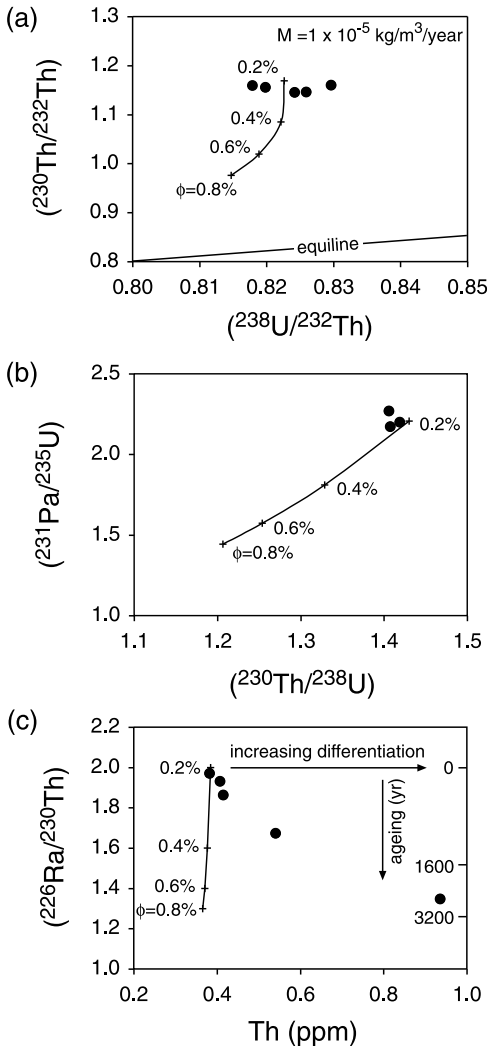

Figure 1. (a) (^{230}Th/^{232}Th) versus (^{238}U/^{232}Th) showing the Asal Rift data relative to a simple dynamic melting simulation (note the expanded scale of the *x* axis). (b) (^{231}Pa/^{235}U) versus (^{230}Th/^{238}U) with the same melting model as in Figure 1a. (c) (^{226}Ra/^{230}Th) versus Th content showing the melting model as well as vectors for fractional crystallization and aging. Melting model was calculated using the equations given in *Williams and Gill* [1989] with $D_U = 3.97 \times 10^{-3}$, $D_{Th} = 2.06 \times 10^{-3}$, $D_{Pa} = 6.00 \times 10^{-4}$, $D_{Ra} = 4.48 \times 10^{-6}$, $D_{Pb} = 2.33 \times 10^{-2}$ based on *Blundy and Wood* [2003] assuming a 3 Gpa mantle source composed of 55% olivine, 18% orthopyroxene, 15% clinopyroxene and 12% garnet with melting rate (assuming 5% melting at an upwelling rate of 8 mm/year based on the half spreading rate of the Asal Rift). The source was assumed to be in secular equilibrium and to have 5.5 ppb U and 21 ppb Th. M = the melting rate and the variable porosity (ϕ) is indicated by increments along the melting curves.

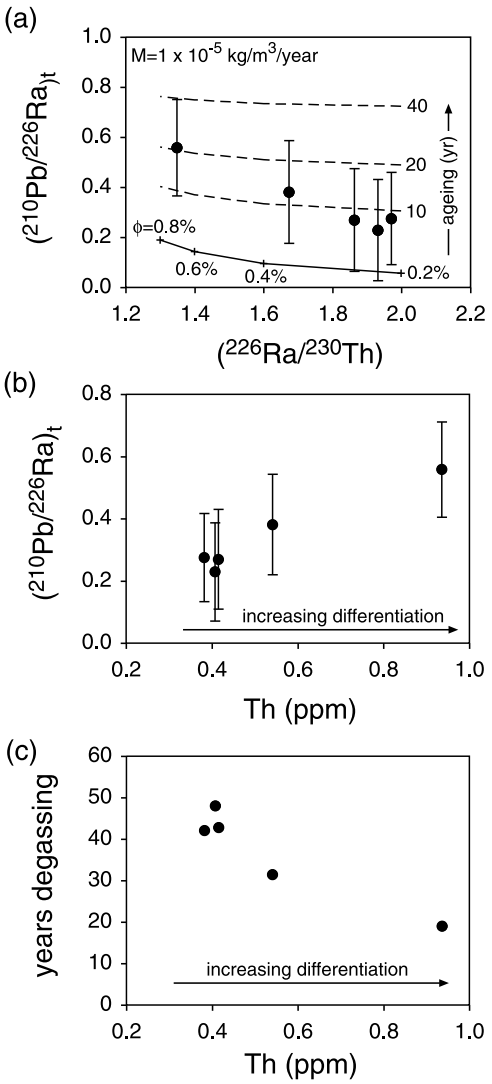

Figure 2. (a) $(^{210}Pb/^{226}Ra)_t$ versus (^{226}Ra/^{230}Th) with the melting model from Figure 1 and dashed curves to indicate the effects of subsequent aging (see text for discussion). (b) $(^{210}Pb/^{226}Ra)_t$ versus Th content permitting that the most evolved lava has the least ^{210}Pb-^{226}Ra disequilibria. (c) Duration of continuous degassing (based on *Gauthier and Condomines* [1999] assuming F = 1) versus Th content suggesting that extent of fractionation may be inversely correlated with the duration of degassing (but see discussion in the text). Error bars in Figures 2a and 2b are 2σ as also discussed in the text.

reconciled if ~10–20 years elapsed between partial melting and eruption (see Figure 2a).

[12] A similar observation was made by *Rubin et al.* [2005] who concluded that their data required melt extraction from the mantle and eruption within a few decades. This would obviously place important constraints on the dynamics of melt movement (see *Dosseto et al.* [2010] for a recent review). Apart from being subaerial and continental, the Asal Rift setting bears similarities with that of the East Pacific Rise and Juan de Fuca Ridge (but not Loihi) and so our new data might be seen to provide new support for the conclusions of *Rubin et al.* [2005]. However, while (^{230}Th/^{238}U) ratios vary in their oceanic basalts, a key aspect of the Asal Rift basalts is that their (^{230}Th/^{238}U), (^{230}Th/^{232}Th), and (^{231}Pa/^{235}U) ratios are essentially invariant (Figures 1a and 1b).

[13] In dynamic melting [e.g., *McKenzie*, 1985; *Williams and Gill*, 1989] or chromatographic porous-flow melting [*Spiegelman and Elliott*, 1993] models, (^{230}Th/^{238}U) ratios are most sensitive to the melting rate whereas (^{231}Pa/^{235}U), (^{226}Ra/^{230}Th) and (^{210}Pb/^{226}Ra) ratios are more sensitive to the porosity of the melting region [*Sims et al.*, 1999; *McKenzie*, 2000; *Elliott and Spiegelman*, 2003]. If the ^{210}Pb deficits of the Asal Rift basalts resulted from partial melting, the magmas must have erupted within decades of formation. As a consequence, any variation in disequilibria among the other nuclide pairs must primarily reflect the melting process. However, if we ascribe the large variation in (^{226}Ra/^{230}Th) ratios in Figure 2a to melting, instead of decay during fractional crystallization (see below), any successful dynamic melting simulation results in a coupled variation, and range in absolute values, of (^{230}Th/^{238}U) and (^{231}Pa/^{235}U). Figures 1a and 1b show that the variations predicted by such models are simply not observed in the data. Moreover, because Ra is more incompatible than Th, progressive melting of a mantle source should cause Th concentrations to decrease along with (^{226}Ra/^{230}Th), which is also the opposite of what is observed. Indeed, there is no melting model that can simultaneously reproduce the variation in the data from all four parent-daughter nuclide pairs (Figures 1 and 2a) in magmas generated from the same source. Therefore we concur with *Vigier et al.* [1999] that the variation in (^{226}Ra/^{230}Th) post-dates partial melting and, by implication, the same must apply for the ^{210}Pb-^{226}Ra disequilibria. Accordingly, mantle partial melting is not the origin of the measured ^{210}Pb deficits, at least in the case of the Asal Rift basalts. In the model illustrated in Figure 1, the combined ^{238}U-^{230}Th, ^{235}U-^{231}Pa and ^{226}Ra-^{230}Th disequilibria reflect a series of melts generated from a relatively homogeneous source under nearly identical conditions (e.g., at a fixed melting rate, porosity, and extent of melting) followed by fractional crystallization over millennia.

6. Fractional Crystallization

[14] At relatively low porosity, the dynamic melting model shown in Figure 1 can simulate the (^{238}U-^{230}Th) and (^{235}U-^{231}Pa) ratios of the Asal Rift basalts (note the highly expanded *x* axis scale). In Figure 1c, the same model can replicate sample (546), which has the highest (^{226}Ra/^{230}Th) ratio and lowest Th concentration (i.e., the least differentiated). This suggests that melt ascent from the mantle occurred sufficiently fast (<8 kyr) to preserve the ^{226}Ra excess in this sample. As discussed and modeled in detail by *Vigier et al.* [1999], the trend toward lower (^{226}Ra/^{230}Th) ratios and higher Th concentrations is consistent with 30–50% fractional crystallization over a timescale that was (1) insignificant relative to the half-life of ^{230}Th (75 kyr), (2) similar to the half-life of ^{226}Ra (1600 yr) and (3) much longer than the half-life of ^{210}Pb (22.6 yr). The alternative explanation, of lowering the (^{226}Ra/^{230}Th) values and raising Th concentrations in magmas by bulk assimilation of crustal materials, is considered not to be viable because Th and Sr isotopic compositions are homogeneous in the Asal lavas [*Vigier et al.*, 1999]. Thus, although the mantle-melting model predicts both ^{226}Ra excesses and ^{210}Pb deficits in the primary melts, any ^{210}Pb disequilibria would probably have decayed away during ascent and clearly would have been fully erased during the time scales inferred for fractional crystallization. In other words, the ^{210}Pb deficits were generated by a process that post-dates both melt ascent from the mantle and subsequent fractional crystallization. This also precludes the origin of the ^{210}Pb deficits by sulfide fractionation. In any case, sulfide saturation is likely to occur in response to redox changes caused by the onset of magnetite fractionation [*Jenner et al.*, 2010]. Increases in TiO_2 and Au with increasing extent of fractional crystallization in the Asal Rift basalts (not shown) independently indicate that neither magnetite nor sulfide fractionation occurred in these magmas.

7. Interaction With Cumulates?

[15] *Van Orman and Saal* [2009] suggested that a possible explanation of ^{210}Pb deficits in basaltic

magmas lies in diffusive interaction with cumulates in crustal magma chambers. In this model it is the rapid decay of ^{210}Pb and its greater compatibility and more rapid diffusion in plagioclase and clinopyroxene, relative to ^{226}Ra, that results in the potential for cumulates to become an internal sink for ^{210}Pb. Numerical calculations suggest that such a process could, in principle, develop (^{210}Pb/^{226}Ra) ratios <0.5 within a few decades [*Van Orman and Saal*, 2009]. In practice, such models remain hard to test in individual magmas not least because chromatographic effects during porous flow through crystals with which they are in equilibrium have little effect on overall magma compositions [e.g., *Navon and Stolper*, 1987]. For the Asal Rift lavas, we consider it highly unlikely that their ^{210}Pb deficits result from magma – cumulate interaction for the following reasons. First, different levels of crystal fractionation from nearly identical parent magmas explains the variation in the bulk compositions of the Asal basalts, and most if not all of this crystal fractionation and crystal liquid separation occurred prior to the generation of the measured ^{210}Pb deficits. Second, interaction between magmas migrating through interconnected pores in plagioclase-rich cumulates derived from similar magmas should produce (^{210}Pb) < (^{226}Ra) < (^{230}Th) rather than the observed (^{210}Pb) < (^{226}Ra) > (^{230}Th). Clinopyroxene rich cumulates could produce the correct sequence of relative activities, but would not have the leverage to produce the large ^{210}Pb deficits seen in the Asal lavas. Third, the greatest ^{210}Pb deficits are found in the Asal lavas with the greatest enrichments in Sr and Eu and thus the greatest amount (~30%) of accumulated plagioclase [*Vigier et al.*, 1999]. According to the *Van Orman and Saal* [2009] model, plagioclase should have significant ^{210}Pb excess such that plagioclase accumulation would mitigate any original ^{210}Pb deficits in these lavas and potentially impart ^{210}Pb excesses. We observe the opposite.

8. Degassing

[16] The decrease of (^{226}Ra/^{230}Th) toward secular equilibrium with increasing fractional crystallization in the Asal Rift basalts in Figure 1c is similar to many other intravolcano U-series data sets [e.g., *Blake and Rogers*, 2005]. Figure 2b shows that (^{210}Pb/^{226}Ra)$_t$ broadly increases toward secular equilibrium with increasing fractional crystallization in these rocks (cf. the most evolved magmas were erupted first). As discussed above, the very different half-lives of these two nuclide pairs requires that these reflect different processes. Since neither partial melting or interaction with cumulates can readily explain the Asal rift ^{210}Pb-^{226}Ra disequilibria and the latter must have formed after millennial scale fractional crystallization, we infer that the ^{210}Pb deficits result from magma degassing subsequent to differentiation. It is possible that differentiation occurred at depth and degassing occurred in the magma chamber imaged 2–4 km beneath the rift.

[17] Using the formulation of *Gauthier and Condomines* [1999], we estimate that the Asal Rift basalts underwent degassing for at least 20–50 years prior to eruption (Table 1). Note that these calculations assume 100% efficient, continuous degassing of ^{222}Rn and that less efficient degassing would increase these estimated durations. Figure 2c shows that the inferred duration of degassing may decrease with increasing fractional crystallization. Unfortunately, the errors on the (^{210}Pb/^{226}Ra)$_t$ values in the basalts propagated for the age of eruption (cf. Figures 2a and 2b) preclude a definitive statement about the relative degassing timescales or degassing efficiencies for the more and less differentiated lavas. Nevertheless, when combined with other observations there appear to be some generalities emerging from ^{210}Pb systematics, as we now discuss.

9. Wider Implications

[18] The best explanation for the ^{210}Pb deficits with respect to ^{226}Ra in the Asal Rift basalts is that their magmas degassed for two to five decades before they erupted. Similar deficits have been documented in basaltic lavas from continental [e.g., *Chakrabarti et al.*, 2009] and oceanic [*Rubin et al.*, 2005] rift environments and even in some subduction related lavas [e.g., *Turner et al.*, 2004]. Thus, there is a growing body of literature suggesting that basalts can degas persistently for decades before they erupt. This degassing could be related to depressurization and slow segregation of CO_2, H_2O, SO_2 and other volatile species as the magmas rise toward the surface. By implication, the same might be true of the oceanic basalts discussed in *Rubin et al.* [2005] and those from the East Pacific Rise appear to be CO_2 super-saturated and may therefore have been undergoing prolonged degassing.

[19] It has been suggested that even highly voluminous magmas may assemble only decades prior to eruption [e.g., *Druitt et al.*, 2012]. Since degassing will inevitably lead to crystallization [e.g., *Cashman*

and Blundy, 2000; *Brophy*, 2009] it is, in principle, also possible that degassing and fractional crystallization might be linked. Our new data from the Asal basalts are similar to results from previous studies of Vestmannaeyjar volcano in Iceland [*Sigmarsson*, 1996] and Sangeang Api in Indonesia [*Turner et al.*, 2004], in that it is the early erupted ± more differentiated magmas from single eruptions that have the higher (^{210}Pb/^{226}Ra) ratios. This is the opposite of what would be expected if degassing promotes crystallization. The evidence at Asal is that fractional crystallization occurred prior to degassing and such observations are not restricted to extensional settings. For example, *Turner et al.* [2004] reported ^{210}Pb deficits from Sangeang Api volcano in the Sunda arc where differentiation is inferred to have occurred over millennia [*Turner et al.*, 2003].

[20] In this scenario, inferred correlations between the calculated duration of degassing and the degree of fractional crystallization (e.g., Figures 2b and 2c) do not require that these two processes are coupled. Rather, it may be that a common result of magmatic plumbing systems is that gas accumulates in the more differentiated magmas that reside at the top of magma reservoirs and are the first to erupt. In some instances, such gas accumulation can even lead to these magmas having ^{210}Pb excesses like those observed at Arenal volcano [*Reagan et al.*, 2006]. We infer that the Asal Rift magmas rose toward the surface and ponded for 1–3 decades [e.g., *Gauthier and Condomines*, 1999] before eruption. The uppermost, more differentiated magmas were fluxed by gas from below, reducing their ^{210}Pb deficits. Another possibility is that the more differentiated magmas degassed less efficiently. Either way, the degassing timescales are clearly longer than, and therefore unrelated to, the week-long period of eruption and subsequent months of seismicity. Both of these magmatic processes occurred on significantly shorter timescales than the development of the bulk compositional variation within the magmas that was established by fractional crystallization over the preceding millennia.

Acknowledgments

[21] We are grateful to Kim Berlo and heather Handley for many discussions about ^{210}Pb disequilibria and to Jim Gill and Jim Van Orman for their constructive reviews. This work was directly funded by Australian Research Council Discovery Proposal DP0988658 to S.T. and M.R. and used instrumentation funded by ARC LIEF and DEST Systemic Infrastructure Grants, Macquarie University and Industry. M.R. also thanks NSF grant EAR 0738776 for support. This is GEMOC publication 188/831.

References

Berlo, K., and S. Turner (2010), Origins of ^{210}Pb-^{226}Ra disequilibria in young volcanic rocks, *Earth Planet. Sci. Lett.*, *296*, 155–164, doi:10.1016/j.epsl.2010.05.023.

Berlo, K., S. Turner, S. Black, C. Hawkesworth, and J. Blundy (2006), Tracing magma degassing prior to eruption using (^{210}Pb/^{226}Ra) disequilibria in volcanic deposits of the 1980–1986 eruptions of Mount St Helens, *Earth Planet. Sci. Lett.*, *249*, 337–349, doi:10.1016/j.epsl.2006.07.018.

Blake, S., and N. Rogers (2005), Magma differentiation rates from (^{226}Ra/^{230}Th) and the size and power output of magma chambers, *Earth Planet. Sci. Lett.*, *236*, 654–669, doi:10.1016/j.epsl.2005.05.035.

Blundy, J. D., and B. J. Wood (2003), Mineral-melt partitioning of uranium-thorium and their daughters, *Rev. Mineral. Geochem.*, *52*, 59–123, doi:10.2113/0520059.

Brophy, J. G. (2009), Decompression and H_2O exsolution driven crystallization and fractionation: Development of a new model for low-pressure fractional crystallization in calc-alkaline magmatic systems, *Contrib. Mineral. Petrol.*, *157*, 797–811, doi:10.1007/s00410-008-0365-2.

Cashman, K., and J. Blundy (2000), Degassing and crystallization of ascending andesite and dacite, *Philos. Trans. R. Soc. London*, *358*, 1487–1513, doi:10.1098/rsta.2000.0600.

Chakrabarti, R., K. W. W. Sims, A. R. Basu, M. Reagan, and J. Durieux (2009), Timescales of magmatic processes and eruption ages of the Nyiragongo volcanics from ^{238}U-^{230}Th-^{226}Ra-^{210}Pb disequilibria, *Earth Planet. Sci. Lett.*, *288*, 149–157, doi:10.1016/j.epsl.2009.09.017.

Condomines, M., O. Sigmarsson, and P.-J. Gauthier (2010), A simple model of ^{222}Rn accumulation leading to ^{210}Pb excesses in volcanic rocks, *Earth Planet. Sci. Lett.*, *293*, 331–338, doi:10.1016/j.epsl.2010.02.048.

Dosseto, A., S. P. Turner, and J. A. Van Orman (2010), *Timescales of Magmatic Processes: From Core to Atmosphere*, 264 pp., John Wiley, Chichester, U. K.

Druitt, T. H., F. Costa, E. Deloule, M. Dungan, and B. Scaillet (2012), Decadal to monthly timescales of magma transfer and reservoir growth at a caldera volcano, *Nature*, *482*, 77–80, doi:10.1038/nature10706.

Elliott, T., and M. Spiegelman (2003), Melt migration in oceanic crustal production: A U-series perspective, in *Treatise on Geochemistry*, vol. 3, *The Crust*, pp. 465–510, Elsevier, Oxford, U. K., doi:10.1016/B0-08-043751-6/03031-0.

Gauthier, P.-J., and M. Condomines (1999), ^{210}Pb-^{226}Ra radioactive disequilibria in recent lavas and radon degassing: Inferences on the magma chamber dynamics at Stromboli and Merapi volcanoes, *Earth Planet. Sci. Lett.*, *172*, 111–126, doi:10.1016/S0012-821X(99)00195-8.

Jacques, E., G. C. P. King, P. Tapponnier, J. C. Ruegg, and I. Manighetti (1996), Seismic activity triggered by stress changes after the 1978 events in the Asal Rift, Djibouti, *Geophys. Res. Lett.*, *23*, 2481–2484, doi:10.1029/96GL02261.

Jenner, F. E., H. S. C. O'Neill, R. J. Arculus, and J. A. Mavrogenes (2010), The magnetite crisis in the evolution of arc-related magmas and the initial concentration of Au, Ag and Cu, *J. Petrol.*, *51*, 2445–2464, doi:10.1093/petrology/egq063.

McKenzie, D. (1985), ^{230}Th-^{238}U disequilibrium and the melting processes beneath ridge axes, *Earth Planet. Sci. Lett.*, *72*, 149–157, doi:10.1016/0012-821X(85)90001-9.

McKenzie, D. (2000), Constraints on melt generation and transport from U-series activity ratios, *Chem. Geol.*, *162*, 81–94, doi:10.1016/S0009-2541(99)00126-6.

Navon, O., and E. Stolper (1987), Geochemical consequences of melt percolation: The upper mantle as a chromatographic column, *J. Geol.*, *95*, 285–307, doi:10.1086/629131.

Reagan, M. K., F. J. Tepley III, J. B. Gill, M. Wortel, and B. Hartman (2005), Rapid time scales of basalt to andesite differentiation at Anatahan volcano, Marian Islands, *J. Volcanol. Geotherm. Res.*, *146*, 171–183, doi:10.1016/j.jvolgeores.2004.10.022.

Reagan, M. K., F. J. Tepley III, J. B. Gill, M. Wortel, and J. Garrison (2006), Timescales of degassing and crystallization implied by ^{210}Po-^{210}Pb-^{226}Ra disequilibria for andesitic lavas erupted from Arenal volcano, *J. Volcanol. Geotherm. Res.*, *157*, 135–146, doi:10.1016/j.jvolgeores.2006.03.044.

Rubin, K. H., I. van der Zander, M. C. Smith, and E. C. Bergmanis (2005), Minimum speed limit for ocean ridge magmatism from ^{210}Pb-^{226}Ra-^{230}Th disequilibria, *Nature*, *437*, 534–538, doi:10.1038/nature03993.

Sigmarsson, O. (1996), Short magma residence time at an Icelandic volcano inferred from U-series disequilibria, *Nature*, *382*, 440–442, doi:10.1038/382440a0.

Sims, K. W. W., D. J. DePaolo, M. T. Murrell, W. S. Baldridge, S. Goldstein, D. Clague, and M. Jull (1999), Porosity of the melting zone and variations in the solid mantle upwelling rate beneath Hawaii: Inferences from ^{238}U-^{230}Th-^{226}Ra and ^{235}U-^{231}Pa disequilibria, *Geochim. Cosmochim. Acta*, *63*, 4119–4138, doi:10.1016/S0016-7037(99)00313-0.

Spiegelman, M., and T. Elliott (1993), Consequences of melt transport for uranium series disequilibrium in young lavas, *Earth Planet. Sci. Lett.*, *179*, 581–593.

Turner, S., B. Bourdon, C. Hawkesworth, and P. Evans (2000), ^{226}Ra-^{230}Th evidence for multiple dehydration events, rapid melt ascent and the time scales of differentiation beneath the Tonga-Kermadec island arc, *Earth Planet. Sci. Lett.*, *179*, 581–593, doi:10.1016/S0012-821X(00)00141-2.

Turner, S., J. Foden, R. George, P. Evans, R. Varne, M. Elburg, and G. Jenner (2003), Rates and processes of potassic magma generation at Sangeang Api volcano, east Sunda arc, Indonesia, *J. Petrol.*, *44*, 491–515, doi:10.1093/petrology/44.3.491.

Turner, S., S. Black, and K. Berlo (2004), ^{210}Pb-^{226}Ra and ^{232}Th-^{228}Ra systematics in young arc lavas: Implications for magma degassing and ascent rates, *Earth Planet. Sci. Lett.*, *227*, 1–16, doi:10.1016/j.epsl.2004.08.017.

Turner, S., K. W. W. Sims, M. Reagan, and C. Cook (2007), A ^{210}Pb-^{226}Ra-^{230}Th-^{238}U study of Klyuchevskoy and Bezymianny volcanoes, Kamchatka, *Geochim. Cosmochim. Acta*, *71*, 4771–4785, doi:10.1016/j.gca.2007.08.006.

Van Ngoc, P., D. Boyer, J.-L. Le Mouel, and V. Courtillot (1981), Identification of a magma chamber in the Ghoubbet-Asal Rift (Djibouti) from a magnetotelluric experiment, *Earth Planet. Sci. Lett.*, *52*, 372–380, doi:10.1016/0012-821X(81)90190-4.

Van Orman, J. A., and A. E. Saal (2009), Influence of crustal cumulates on ^{210}Pb disequilibria in basalts, *Earth Planet. Sci. Lett.*, *284*, 284–291, doi:10.1016/j.epsl.2009.04.034.

Vigier, N., B. Bourdon, J. L. Joron, and C. J. Allègre (1999), U-decay series and trace element systematics in the 1978 eruption of Ardoukoba, Asal rift: Timescale of magma crystallization, *Earth Planet. Sci. Lett.*, *174*, 81–98, doi:10.1016/S0012-821X(99)00256-3.

Williams, R. W., and J. B. Gill (1989), Effects of partial melting on the uranium decay series, *Geochim. Cosmochim. Acta*, *53*, 1607–1619, doi:10.1016/0016-7037(89)90242-1.